NASA
Technical
Paper
2459

April 1985

An Electrochemical Study of the Corrosion Behavior of Primer Coated 2219-T87 Aluminum

Merlin D. Danford
and Ralph H. Higgins

NASA

NASA Technical Paper 2459

1985

An Electrochemical Study of the Corrosion Behavior of Primer Coated 2219-T87 Aluminum

Merlin D. Danford
and Ralph H. Higgins

George C. Marshall Space Flight Center
Marshall Space Flight Center, Alabama

National Aeronautics
and Space Administration

Scientific and Technical Information Branch

TABLE OF CONTENTS

LIST OF ILLUSTRATIONS

LIST OF TABLES

TECHNICAL PAPER

AN ELECTROCHEMICAL STUDY OF THE CORROSION BEHAVIOR OF PRIMER COATED 2219-T87 ALUMINUM

INTRODUCTION

This study was directed toward the investigation and development of electrochemical methods for assessing the corrosion of painted metals, with special emphasis on the primers employed for the External Tank and Solid Rocket Boosters of the Space Shuttle System. Previous work in this area has been described in a review article by Wolstenholme [1]. This work included many potential-time and potential-current measurements. A great deal of attention has been received by the work of Wormwell and Brasher [2], who investigated the effects of surface preparation and the type and number of coats of paint on the potential of coated steel specimens immersed in synthetic seawater, using paints intended for total immersion conditions on ship hulls. Figure 1 shows a typical curve plotted from mean values for a considerable number of specimens. The beginning of the gradual decline in potential following the peak coincided with the onset of rusting, indicated by the corresponding corrosion weight loss. It was concluded from this that the period required to pass the peak represented the useful life of the paint, and that this period was extended in proportion to the weight of paint applied per unit area.

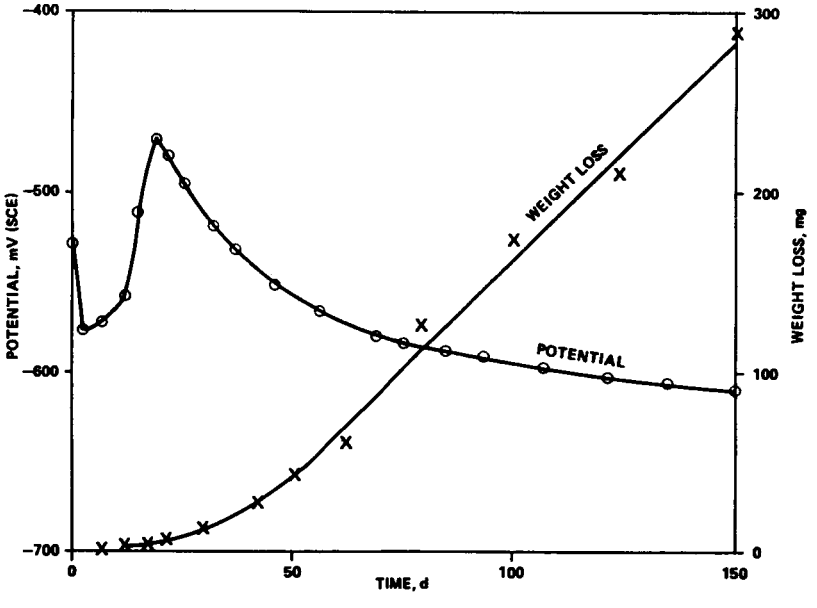

Figure 1. Potential-time and weight loss curves for painted steel from Wormwell and Brasher.

Apparently no electrical resistance-time studies have previously been made. However, some interesting observations on coating porosity related to resistance and potential were made by Yakubovitch, et al. [3]. Paint films with thicknesses below a certain critical value showed abnormally low electrical resistances due, it was said, to an increased number of pores and defects in the thinner films. This was also reflected in the measured potential values for painted steel, which were relatively negative for very thin coatings, increasing sharply when the thickness exceeded the critical value.

Investigations of paint films using polarization measurements include the work of Bureau [4] and Rozenfel'd, et al. [5]. Corrections for ohmic drop due to the paint films were made in both of these studies. Bureau potentiokinetically polarized painted specimens to ±100 mV from the rest potential, and the gradient of the current-potential curve, $\Delta E/\Delta I$, described as the polarization resistance, was stated to be inversely proportional to the corrosion rate of the metal. It was said that the measured values of the polarization resistance were independent of the thickness of the paint films and that the polarization resistance was much higher than the ionic resistance of the paint film. Measurements by Rozenfel'd, et al. indicated that polarization resistance accounted for 95 to 98 percent of the total resistance of the system and only 2 to 5 percent was due to ohmic resistance.

In the present study, potential-time, resistance-time and polarization resistance techniques were all investigated in order to evaluate the effectiveness of various primers in protecting 2219-T87 aluminum from corrosion. This is the material used for construction of the External Tank and most of the forward and aft structures of the Solid Rocket Boosters of the Space Shuttle System.

THE EFFECT OF UNCOMPENSATED IR-DROP ON POLARIZATION RESISTANCE MEASUREMENTS

A theoretical analysis of the effect of uncompensated IR-drop on polarization resistance (R_p) measurements has been given by Mansfeld [6]. The basis for electrochemical determination of corrosion rates is the relationship between external (measured) current (I_s) and potential (ϕ) or polarization ($\Delta\phi = \phi - \phi_{CORR}$) in the form:

$$I_s = I_{CORR} \left\{ \exp\left(\frac{\Delta\phi}{b_a'}\right) - \exp\left(-\frac{\Delta\phi}{b_c'}\right) \right\} \tag{1}$$

Here, b_a' and b_c' are the anodic and cathodic Tafel slopes, respectively. Tafel slopes are defined as shown in Figure 2. When a controlled potential scan is applied to a sample starting several millivolts below

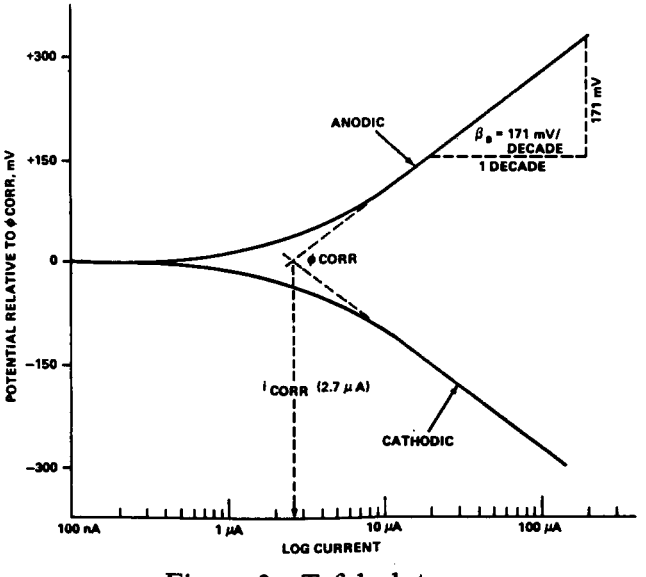

Figure 2. Tafel plot.

ϕ_{CORR}, the corrosion potential, and extending to several millivolts above ϕ_{CORR}, a plot of the function on semi-log paper characteristically exhibits a linear region. This is true for both anodic and cathodic plots. The plot itself is known as a Tafel Plot and the slope of the linear region in V/decade or mV/decade is known as the Tafel Slope.

The corrosion current (I_{CORR}) can be obtained by extrapolation of anodic and cathodic Tafel lines to the corrosion potential (ϕ_{CORR}) or by measurement of the polarization resistance (R_p) defined as:

$$\left(\frac{\delta\,\Delta\phi}{\delta\,I_s}\right)_{\Delta\phi=0} = R_p = \frac{1}{I_{CORR}}\left[\frac{1}{b_a'} - \frac{1}{b_c'}\right]^{-1} \tag{2}$$

The dimension of R_p as defined in equation (2) is ohm·cm^2, and I_{CORR} is the corrosion current density. The total area of sample exposed in the present study was 1.0 cm^2, so that R_p is expressed directly in ohms in this case. In the presence of a resistance (R_Ω) between the reference electrode and the metal sample surface, the measured relationship between current (I_s) and the polarization ($\Delta\phi$) is distorted since the measured polarization ($\Delta\phi'$) now contains a contribution from IR-drop ($\Delta\phi' = \Delta\phi - I_s R_\Omega$). The current-potential relationship for this case can be expressed as:

$$I_s = I_{CORR}\left\{\exp\left(\frac{\Delta\phi'}{b_a}\right) - \exp\left(-\frac{\Delta\phi'}{b_c}\right)\right\} \tag{3}$$

If the quantity B is defined as:

$$B = \left(\frac{1}{b_a'} + \frac{1}{b_c'}\right)^{-1} = \frac{b_a\,b_c}{2.303(b_a+b_c)} \tag{4}$$

Then, where compensation for IR-drop is applied:

$$I_{CORR} = \frac{B}{R_p} \tag{5}$$

and, where correction for IR-drop is not applied:

$$I_{CORR}' = \frac{B'}{R_p'} \tag{6}$$

Although the derivation will not be shown here, Mansfeld [6] has shown that:

$$R_p' = R_p + R_\Omega \tag{7}$$

The error in determining the corrosion current due to lack of compensation for IR-drop can be expressed as:

$$\delta = \frac{I_{CORR} - I'_{CORR}}{I'_{CORR}} = 1 - \frac{B}{B'} \frac{(R_p+R_\Omega)}{R_p} \tag{8}$$

Equation (8) differs from that derived by Mansfeld in that the quantities B and B′ are included in the present case, but were neglected by Mansfeld. If B = B′, equation (8) reduces to:

$$\delta = \frac{R_\Omega}{R_p} \tag{9}$$

which was the relation derived by Mansfeld. B′ may be quite different from B, as evidenced by results obtained in this study, so that the error from lack of correction for IR-drop may be quite different from that predicted by equation (9).

In the present study, the program PϕLCURR[7] was used for least squares determination of the polarization resistance (R_p), b_a and b_c, I_{CORR} and ϕ_{CORR} using equations (2) and (3). Separate determinations were made, with and without correction for IR-drop, for 0.01N, 0.1N and 1.0N solutions of HCl/EtOH. The same experiment was performed by Mansfeld. The present experiment differs in that type 1010 steel was used as the specimen, whereas iron was used in the previous study. Since the IR-drop in this case is due to the solution only, the values of R_Ω should be the same in both studies, but values of R_p and R_p' will differ. Values of b_a and b_c were not determined in the previous study. IR-drop was measured in the present case with EG&G-PARC Model 356 IR Compensation Module, in conjunction with the EG&G-PARC Model 350A Corrosion Measurement Console. Compensation for IR-drop from the measured resistances were made, where appropriate, during playback of the data after collection. A plot of polarization resistance data with and without correction for IR-drop is shown in Figure 3 for the 0.1N HCl/EtOH solution and a summary of the values of R_Ω, R_p, R_p', R_p+R_Ω and error for lack of correction for IR-drop (δ) is given in Table 1. As seen from Table 1, the values of R_Ω obtained in the present study are in good agreement with those obtained by Mansfeld.

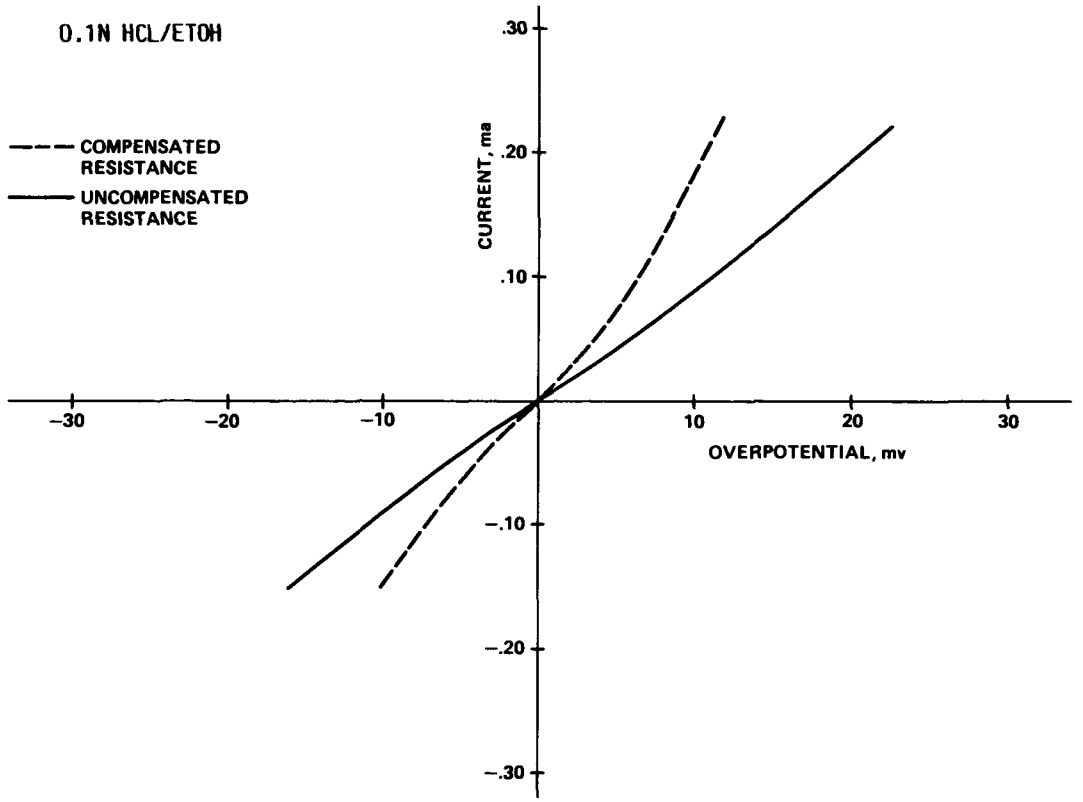

Figure 3. Experimental polarization curve for 1010 steel in 0.1N HCl/EtOH with and without IR-drop compensation.

TABLE 1. POLARIZATION RESISTANCE MEASUREMENTS FOR 1010 STEEL/HCl/EtOH

[HCl]	R_Ω *	R_Ω **	Rp	R'p	$Rp+R_\Omega$	δ
0.01N	212	189	330	529	518	22%
0.1N	42	45	98	119	143	61%
1.0N	8.5	3.1	9.9	13.2	13.0	4.3%

* Reference [6]

** Present Study

EXPERIMENTAL

Measurements of corrosion potentials (ϕ_{CORR}), corrosion rates (obtained with the polarization resistance method), electrical resistances and polarization resistances, also obtained by the polarization resistance technique, were made for 30 days each on several primers applied to 2219-T87 aluminum specimens, which were 1.43 cm in diameter and 0.13 cm thick. The sample holder employed in this study is shown in Figure 4. The painted surface of the sample, with an area of 1.0 cm^2 exposed to the test solution, was immersed for the entire test period in a 3.5 percent NaCl solution, buffered at pH 5.5, in the corrosion cell. An assembled view of the test cell is shown in Figure 5. The exposed sample surface is at the center of the cell, with graphite counter electrodes at the sides and the reference electrode (saturated calomel) at the front. The buffer solution was prepared by mixing 500 ml of 0.1N potassium hydrogen phthalate with 388 ml of 0.1N NaOH and adjusting the total volume to 1 liter. An appropriate weight of NaCl was then added to obtain a 3.5 percent concentration. The relatively low pH (5.5) was chosen to obtain a test medium more corrosive to the aluminum metal substrate, resulting in higher corrosion rates which were more amenable to measurement.

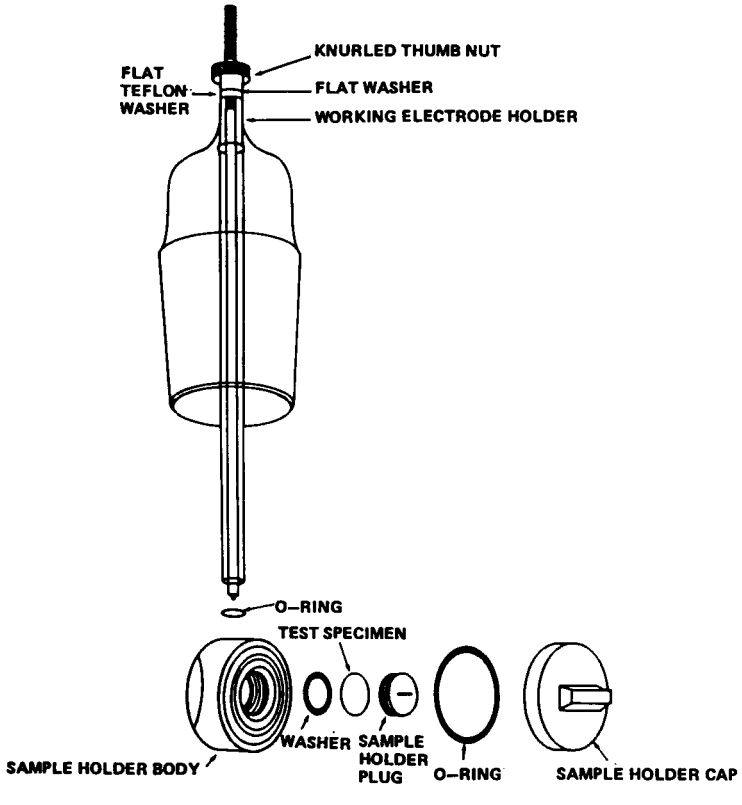

Figure 4. Exploded view of the sample holder.

Sample preparation consisted of a 15 min immersion period of the aluminum specimens in hot alkaline cleaner, followed by a 15 min suspension in Smut-Go chromate deoxidizer. The samples were then treated with Alodine 1200 (conversion coat) for a period of 2 min and sprayed on one side to a measured thickness with the appropriate primer. Sample preparation of primers used for the External Tank of the Space Shuttle System differed in that Iridite 14-2 was used for application of the conversion coat.

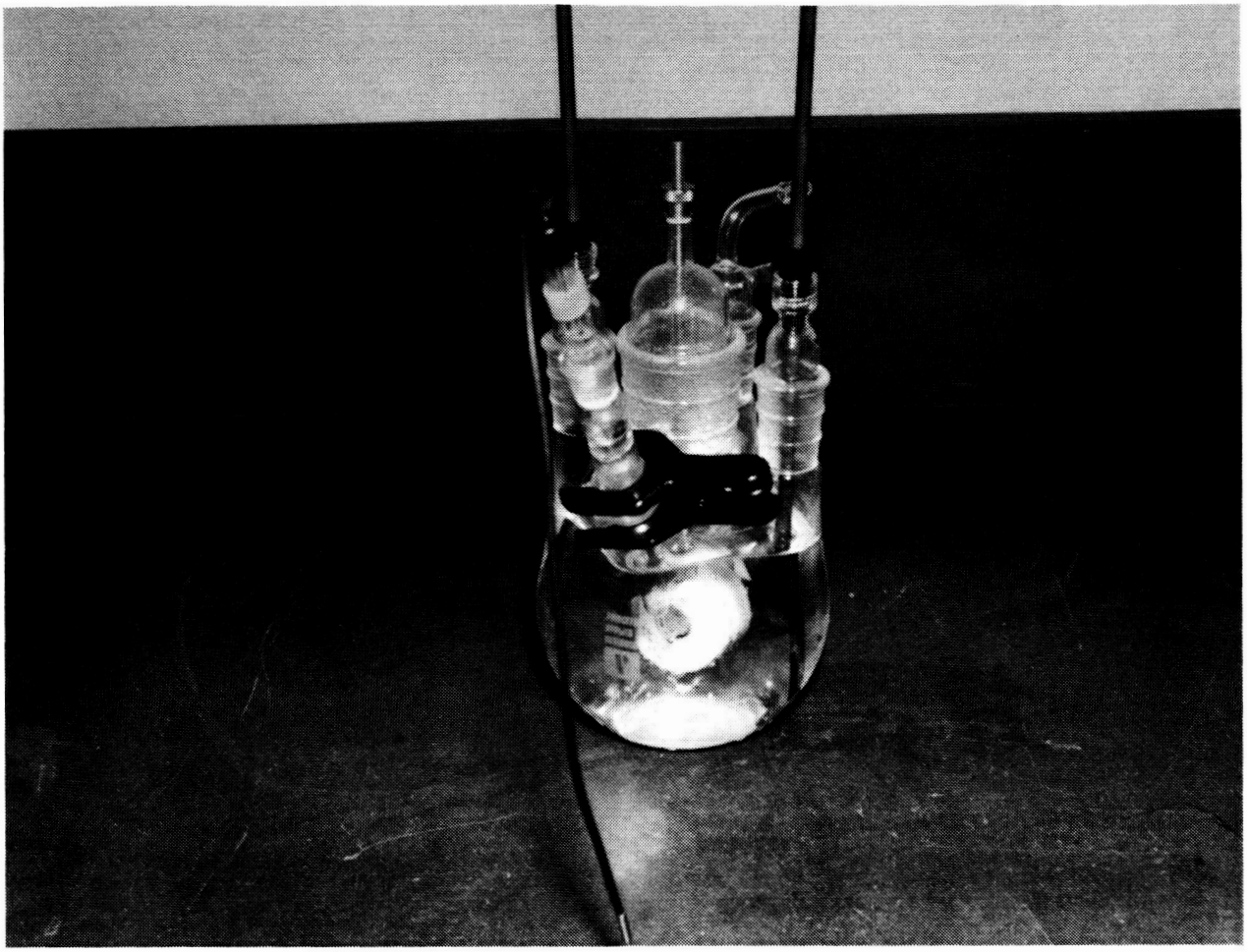

Figure 5. View of the assembled corrosion cell system.

Data for electrical resistances were obtained using the EG&G-PARC Model 356 IR Compensation Module, which has a measurement range from 0.1 ohm to 100,000 ohms, in conjunction with the EG&G-PARC Model 350A Corrosion Measurement Console. Data were collected daily for the first few days for each sample, after which the frequency of data collection was decreased. Values of ϕ_{CORR}, corrosion current (I_{CORR}), and polarization resistance (R_p) were all obtained using the polarization resistance techniques. Data were taken on alternate days with the exception of weekends. The small currents involved in the study of painted surfaces disturb the sample surface very little, so that repeated measurements can be made.

The EG&G-PARC Model 350A Corrosion Measurement Console was used for collection of polarization resistance data. The corrosion cell was immersed in a thermostatically controlled bath at 30°C for each measurement. Data were collected at 0.5 mV intervals at a scan rate of 0.100 mV/sec. The measurement range for all determinations was -20 mV to +20 mV with respect to ϕ_{CORR}. Measurements of the ohmic drop (R_Ω) were then made with the Model 356 IR Compensation Module, and correction for IR-drop was accomplished during playback or transfer of the data to a PDP-11/45 computer which was used for analysis of the data. The data were stored on disk and then transferred to the computer memory for calculation of R_p, ϕ_{CORR}, b_a, b_c and I_{CORR} using the program PϕLCURR[7]. This is a non-linear least squares program using the basic equations (2) and (3) for calculation of the above quantities. For the computer calculations, alternate data points were used, resulting

in a data increment of $\Delta\phi$ = 1.0 mV. I_{CORR} is simply related to the corrosion rate, which is obtained directly from it.

Certain selected primers were chosen for solubility measurements in the test solutions, and one (TT-P-1757 Aerosol) in distilled water. For this purpose, the samples were completely coated with primer. The solubility of primer is likely related to the permeability of the paint film by the test solution and, hence, can be correlated with electrical resistance measurements. The painted samples were weighed to obtain initial weights and immersed in about 80 ml of the test solution for a period of 30 days, with weight measurements being made every 3 or 4 days. At the end of the test period, some of the test solutions were analyzed by atomic absorption spectroscopy for zinc, chromium and aluminum content.

RESULTS AND DISCUSSION

A list of the various aluminum primers investigated is shown in Table 2 together with the vehicles, inhibitors and weight percents of inhibitor in the wet primers. Initial values of the electrical resistances for each thickness of primer are listed in Table 3. All are consistent except for the 35.6-μm thick DeSoto 515-346 primer, where the initial resistance measurement is less than that for the 15.2-μm thick coat. Experience showed that equilibration for a few hours was sometimes necessary to obtain proper values of the initial electrical resistance, and, undoubtedly, insufficient time was allowed before the reading was taken. The resistance for the 35.6-μm thick primer on the second day (18,080 ohms) was greater than that for the 15.2-μm thick primer (14,660 ohms).

TABLE 2. LIST OF PRIMERS INVESTIGATED

Primer	Vehicle	Inhibitor	Wt. Percent $CrO_4^=$
TT-P-1757 (Aerosol)	Alkyd Resin	$ZnCrO_4$	17.9
TT-P-1757 (Air Atomized Spray)	Alkyd Resin	$ZnCrO_4$	17.9
DeSoto 515-346 (Current ET Primer)	Epoxy	$SrCrO_4$	6.0
DeSoto 513-007 (Old ET Primer)	Epoxy	$SrCrO_4$	1.9
Bostik 463-6-3 (SRB Primer)	Epoxy	$CaCrO_4$	<5
MIL-P-23377	Epoxy-Polyamide	$SrCrO_4$	6.8
DeSoto 511-300	Epoxy	Molybdate	---
MIL-P-15930C	Vinyl Resin	$ZnCrO_4$	2.5

TABLE 3. INITIAL VALUES OF R_Ω OBTAINED FOR VARIOUS PRIMERS

Primer	Thickness μm(inches)	Initial R_Ω, ohms
TT-T-1757 (Aerosol)	7.6 (0.0003) 15.2 (0.0006)	270 5,102
TT-P-1757 (Air Atomized Spray)	25.4 (0.0010)	17,300
DeSoto 515-346 (Current ET Primer)	15.2 (0.0006) 35.6 (0.0014)	19,800 17,100*
DeSoto 513-007 (Old ET Primer)	17.8 (0.0007)	30,490
Bostik 463-6-3 (SRB Primer)	25.4 (0.0010)	21,300
MIL-P-23377	27.9 (0.0011)	28,240
DeSoto 511-300 (Molybdate)	22.9 (0.0009) 53.3 (0.0021)	14,070 24,330
MIL-P-15930C	27.9 (0.0011)	31,170

* This value was measured before proper equilibrium was attained.

Values of the initial corrosion rates, for the various chromate primers, as obtained using the polarization resistance method, are listed in Table 4 together with the day on which the corrosion rates became measurable. Generally, the initial corrosion rates are related to the weight percent of $CrO_4^=$ in the primer for primers of comparable thickness, the initial corrosion rates being greater for primers with a lower chromate content. An exception occurred with the Bostik 463-6-3 primer (<5% $Cro_4^=$), where the corrosion rate was not measurable until day 18 and was only 0.0007±0.00004 mils/year (mpy). Corrosion rates less than 0.0006 mpy were not measurable. The electrical resistance-time data for the Bostik 463-6-3 primer, which will be discussed later, show that the primer film is relatively impervious to water, and not appreciably penetrated by the test medium until after about 15 days.

TABLE 4. INITIAL MEASUREMENT TIMES AND CORROSION RATES FOR CHROMATE PRIMERS

Primer	Thickness (μm)	Wt. Percent $CrO4^=$	Time (Days)	Initial Corrosion Rate) (mpy)
TT-P-1757 (Aerosol)	7.6 15.2	17.9 17.9	1 3	0.0128±0.0020 0.0033±0.0010
TT-P-1757 (Air Atomized Spray)	25.4	17.9	---	<0.0006
DeSoto 515-346 (Current ET Primer)	15.2 35.6	6.0 6.0	3 11	0.0191±0.0060 0.0006±0.0001
DeSoto 513-007 (Old ET Primer)	17.8	1.9	2	0.0500±0.0073
Bostik 463-6-3 (SRB Primer)	25.4	<5	18	0.0007±0.00004
MIL-P-23377	27.9	6.8	9	0.0015±0.00004
MIL-P-15930C	27.9	2.5	3	0.0532±0.0037

Normalized resistance-time and corrosion rate-time plots are shown in Figures 6 through 12. The corrosion rate for the TT-P-1757 (air atomized spray) zinc chromate primer was not measurable during the 30 day test period and therefore is not shown in Figure 7. Standard errors for each corrosion rate determined, as obtained with the program PϕLCURR, are also shown in the Figures. Where errors are not shown, they are too small to be displayed. Corrosion potential-time plots showed no significant deviations from the mean values except for the case of the 53.3-μm thick DeSoto 511-300 molybdate primer. Here, the corrosion potential showed an abrupt drop from -230 mV to -800 mV after 26 days. This corresponds with a decrease in electrical resistance and a rise in the corrosion rate, as shown in Figure 6. Corrosion potential-time plots behaved generally as that for the 15.2-μm thick TT-P-1757 aerosol primer, which had a value of -791±5 mV throughout the 30 day test period. Since there are no significant deviations, the corrosion potential-time plots are not shown.

For the purpose of brevity, the normalized electrical resistance-time and corrosion rate-time curves in Figures 6 through 12 will not be individually discussed except for the DeSoto 515-346, the current External Tank primer, DeSoto 513-007, the old External Tank primer, and the Bostik 463-6-3 primer, which is used for the Solid Rocket Boosters of the Space Shuttle Transportation System. These primers are of special interest and will be discussed in one of the following sections. It will be left to the reader to glean information of interest, concerning the other primers, from the various tables and figures presented. The electrical resistance-time curves correlate well with the uptake of water by the paint films, as will be discussed in the following section. The corrosion rate-time curves, in general, show a maximum in the corrosion rate at 14 to 16 days. An exception is the DeSoto 515-346 primer, the primer presently used on the External Tank, which shows a maximum at only 11 days. The correlation of these curves with a proposed corrosion rate mechanism will be described in a later section. The observed corrosion rates depend very significantly on the thickness of the primer. This is also reflected in the polarization resistance values (R_p), these being greater for lower corrosion rates as established

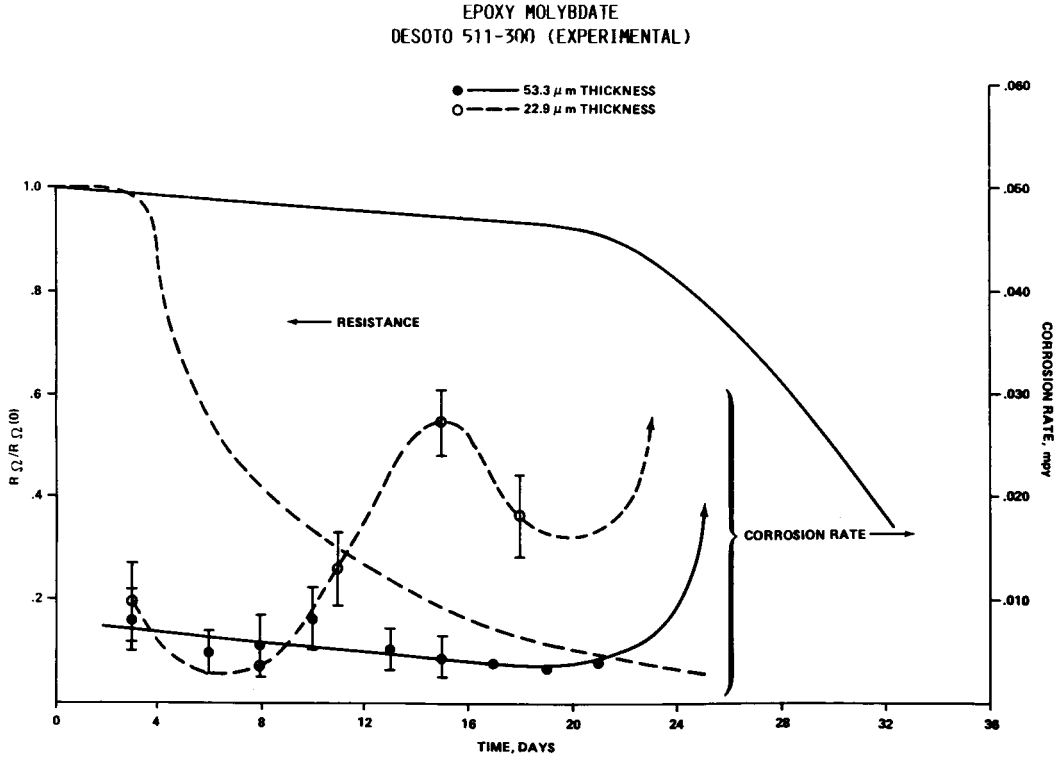

Figure 6. Normalized resistance-time and corrosion rate-time curves for DeSoto 511-300 epoxy molybdate primer.

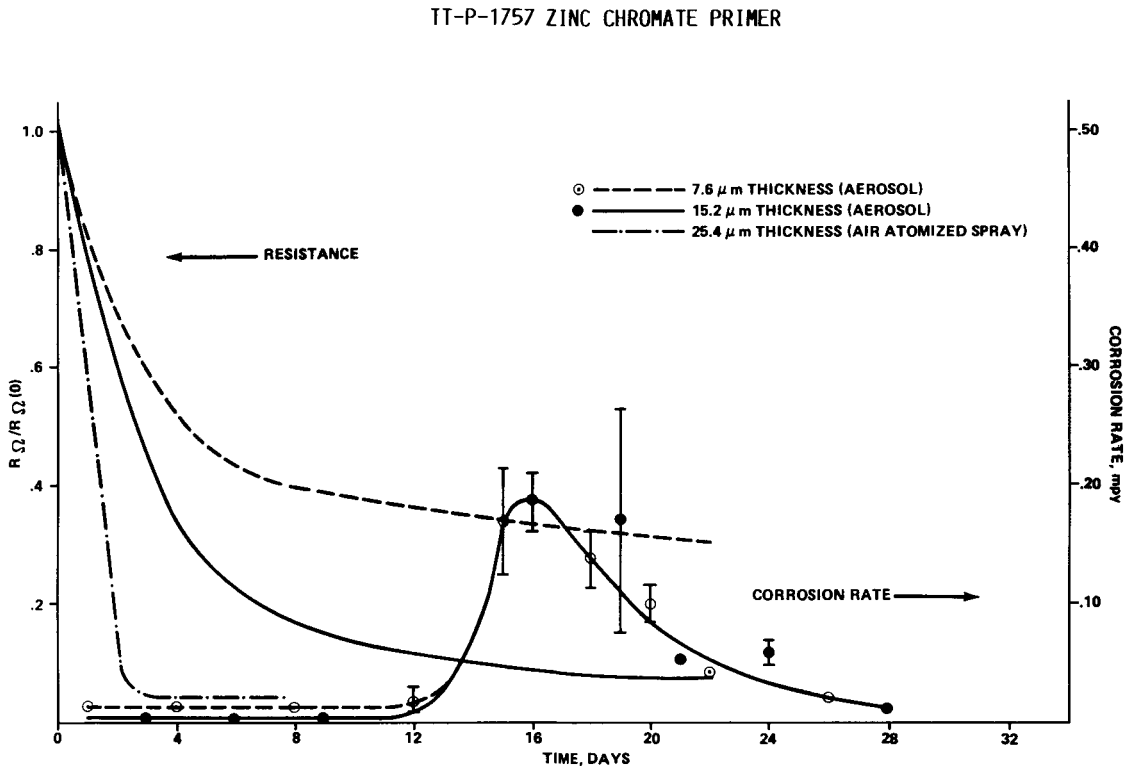

Figure 7. Normalized resistance-time and corrosion rate-time curves for TT-P-1757 primers.

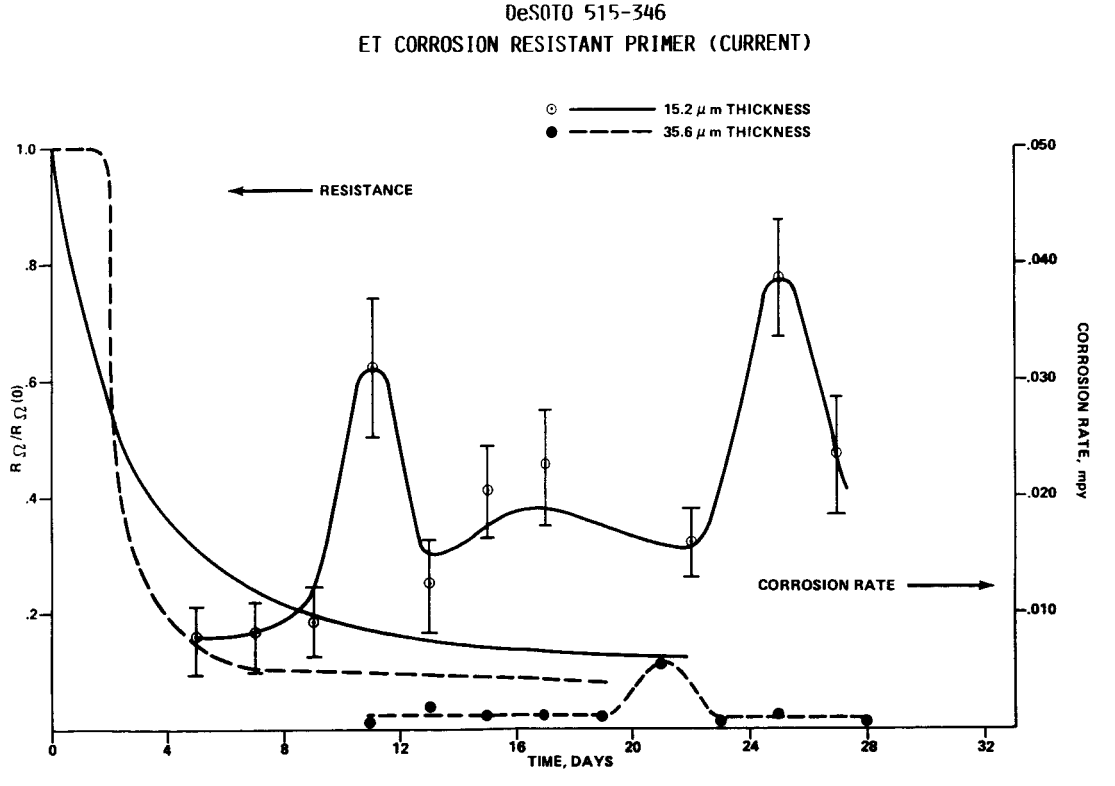

Figure 8. Normalized resistance-time and corrosion rate-time curves for the DeSoto 515-346 primer (present ET primer).

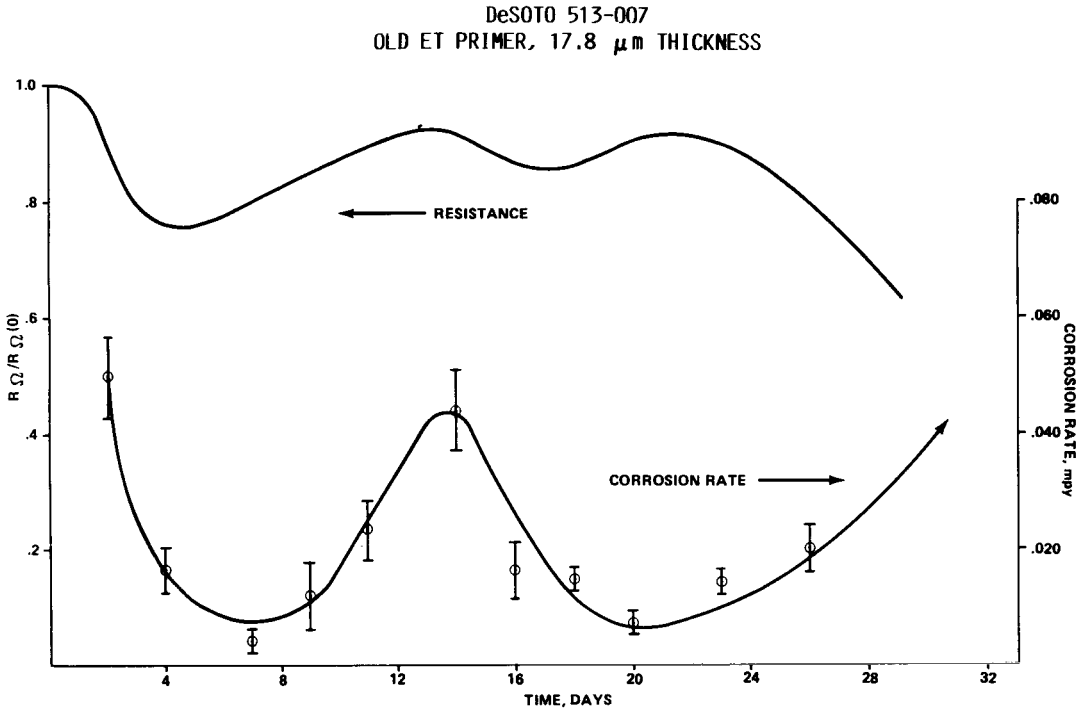

Figure 9. Normalized resistance-time and corrosion rate-time curves for the DeSoto 513-007 Primer (former ET primer).

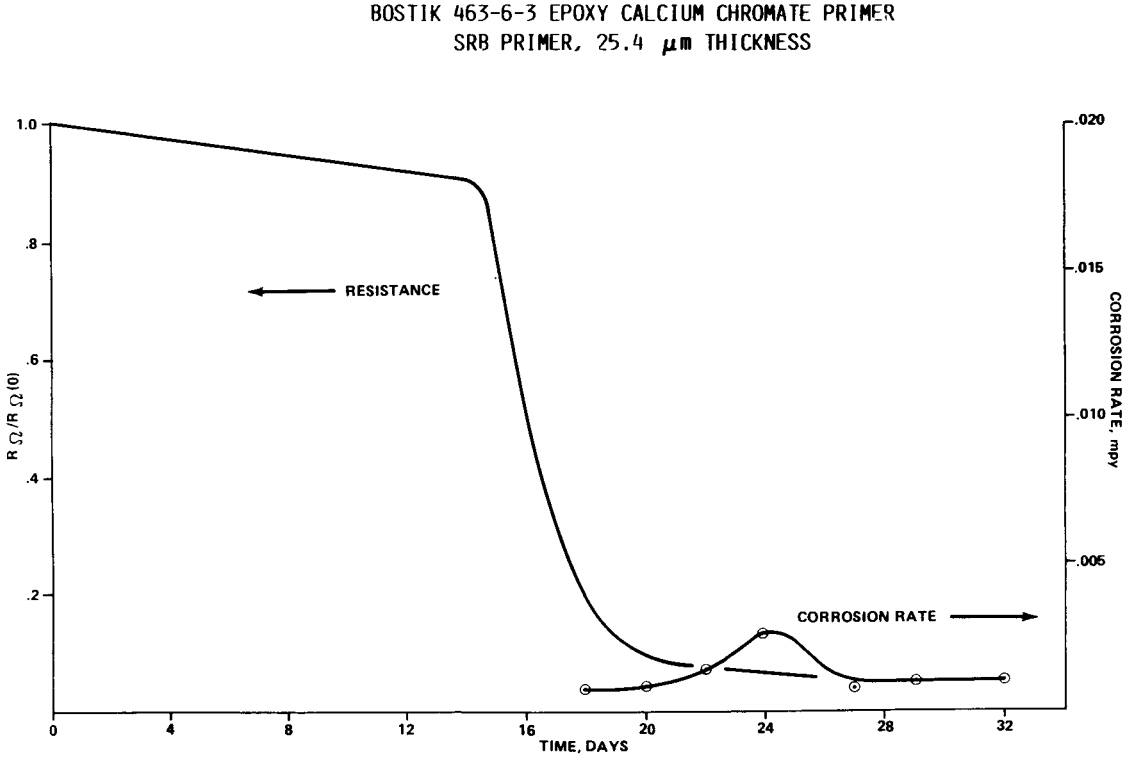

Figure 10. Normalized resistance-time and corrosion rate-time curves for the Bostik 463-6-3 primer (SRB primer).

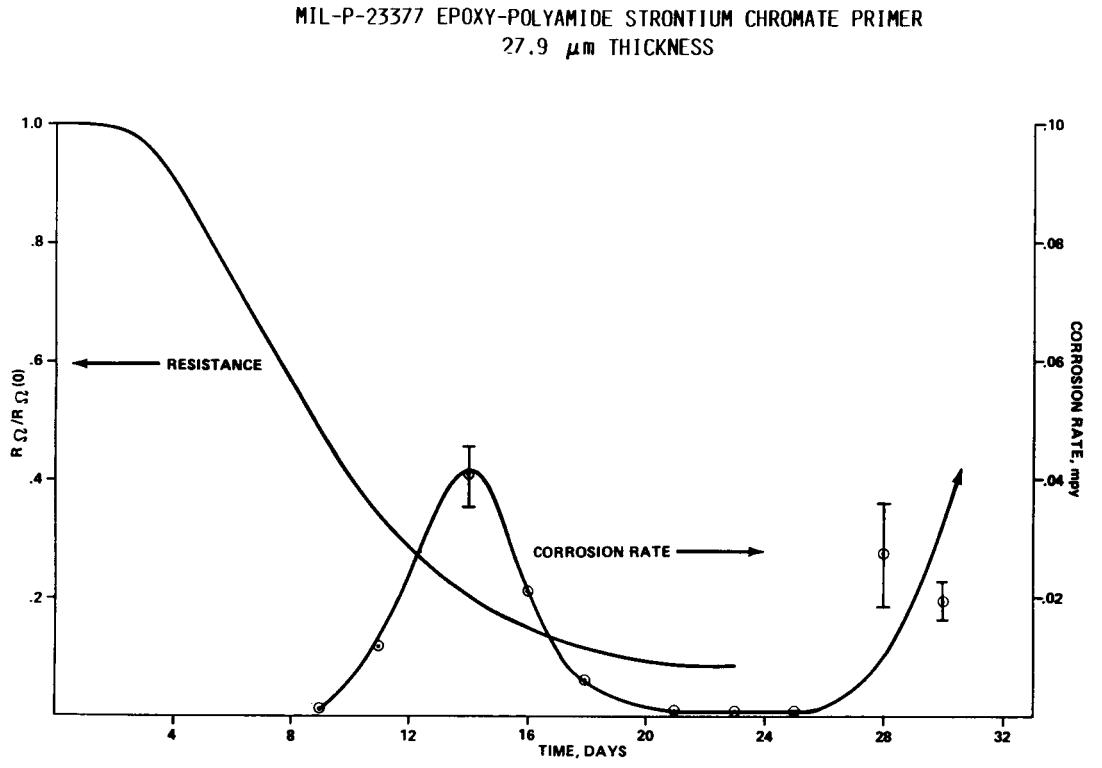

Figure 11. Normalized resistance-time and corrosion rate-time curves for the MIL-P-23377 epoxy-polyamide primer.

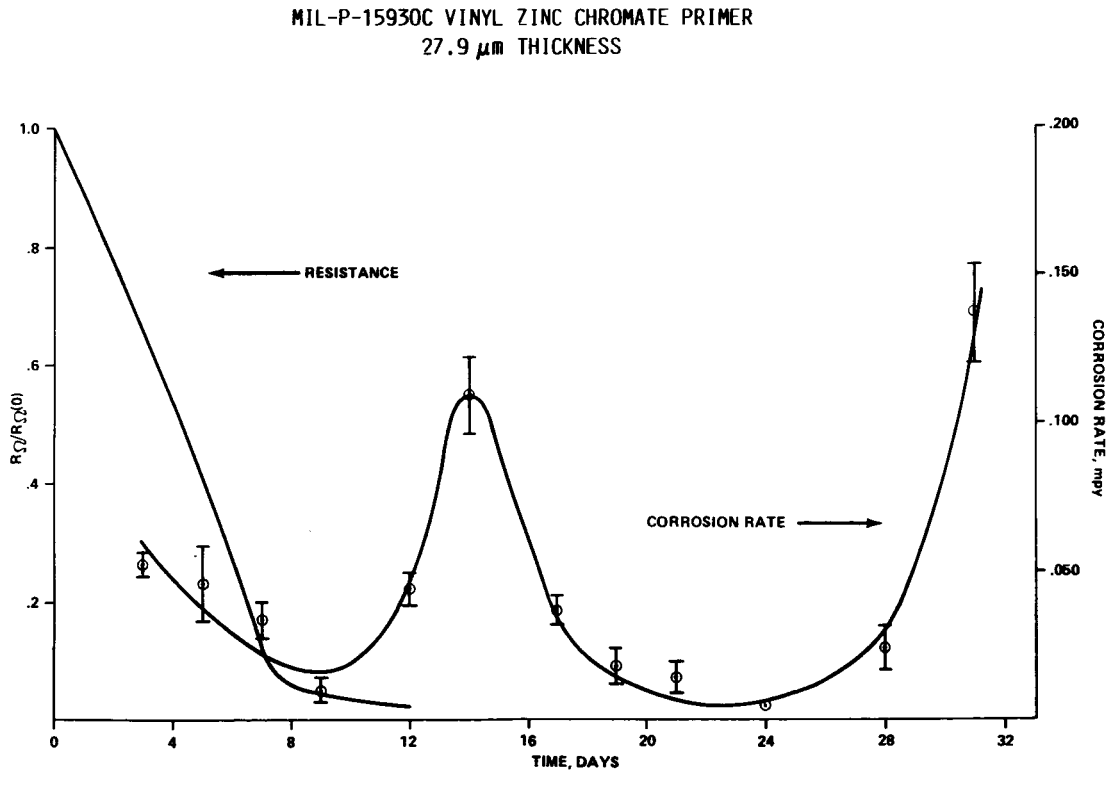

Figure 12. Normalized resistance-time and corrosion rate-time curves for the MIL-P-15930C vinyl resin primer.

through equation (6). In general, plots of R_p versus time showed no significant trends over rather long time periods, but showed marked scatter, as shown in Table 5. The mean values of R_p for designated time periods, together with the mean corrosion rates during these periods are shown in Table 5. These time periods may or may not include the peak in the corrosion rate-time curves. The R_p-time plots showed significant shifts to higher or lower levels after a period of several days, with a corresponding rise or drop in the mean corrosion rates.

TABLE 5. MEAN VALUES WITH STANDARD ERRORS FOR CORROSION RATES AND POLARIZATION RESISTANCE

Primer	Thickness (μm)	Time Interval (Days)	Corrosion Rate (mpy)	Rp (ohms)
TT-P-1757 (Aerosol)	7.6	1-8	0.0131±0.0019	144,400± 6,938
		12-29	0.0767±0.0226	36,686± 4,379
	15.2	3-9	0.0025±0.0004	260,400±44,253
		13-28	0.0830±0.0310	55,460± 9,373
TT-T-1757 (Air Atomized Spray)	25.4	1-30	< 0.0006	-----
DeSoto 515-346 (Current ET Primer)	15.2	3-27	0.0171±0.0025	133,178± 9,360
	35.6	11-28	0.0015±0.0005	817,589±49,952
DeSoto 513-007 (Old ET Primer)	17.8	2-16	0.0277±0.0080	83,260± 3,957
		18-26	0.0143±0.0026	121,553±13,586
Bostik 463-6-3 (SRB Primer)	25.4	18-32	0.0012±0.0002	911,171±114,374
MIL-P-23377	27.9	9-25	0.0123±0.0056	499,050± 96,475
		28-32	0.0240±0.0040	121,553± 13,586
DeSoto 511-300 (Molybdate)	22.9	3-30	0.0307±0.0066	79,774± 8,099
	53.3	1-21	0.0056±0.0007	169,550± 15,942
		25-31	> 0.084	29,263± 6,344
MIL-P-15930C	27.9	3-24	0.0406±0.0100	81,154± 10,760
		28-31	0.0805±0.0566	19,915± 2,955

Correlation of Electrical Resistance-Time Measurements with Water Uptake

For correlation of water uptake with electrical resistance-time curves, the TT-P-1757 zinc chromate primers, both the aerosol and the air atomized spray, were chosen. Figure 13 shows the weight gain versus time for the aerosol primer immersed in distilled water for approximately 30 days. Complete saturation is reached after about 10 days. This correlates well with the drop in the normalized electrical resistance curves shown in Figure 7, where the resistance has dropped to a very low value during this period. A different behavior was observed for a sample immersed in 3.5 percent NaCl solution, as shown in Figure 14. Here, the sample showed a net weight loss extending over the 30 days period due to elution of the primer pigment. A similar behavior was exhibited by the DeSoto 515-346 primer, which is currently used for the External Tank. According to Figure 7, the drop in electrical resistance is much sharper for the TT-P-1757 air atomized spray than for the TT-P-1757 aerosol primer. Reference to Figure 15 reveals that there is an initial weight gain in the case of the air atomized spray for a sample immersed in 3.5 percent NaCl solution, due to a very rapid absorption of water. Thus, the rate of decrease in electrical resistance seems to show good correlation with the rate of water uptake by the primer.

Analysis of the solutions after the 30 day period by atomic absorption spectroscopy showed that $ZnCrO_4$ was being eluted stoichiometrically at pH 5.5, with solubility being enhanced in the 3.5 percent NaCl solutions in accord with the Debye-Hückel limiting law.

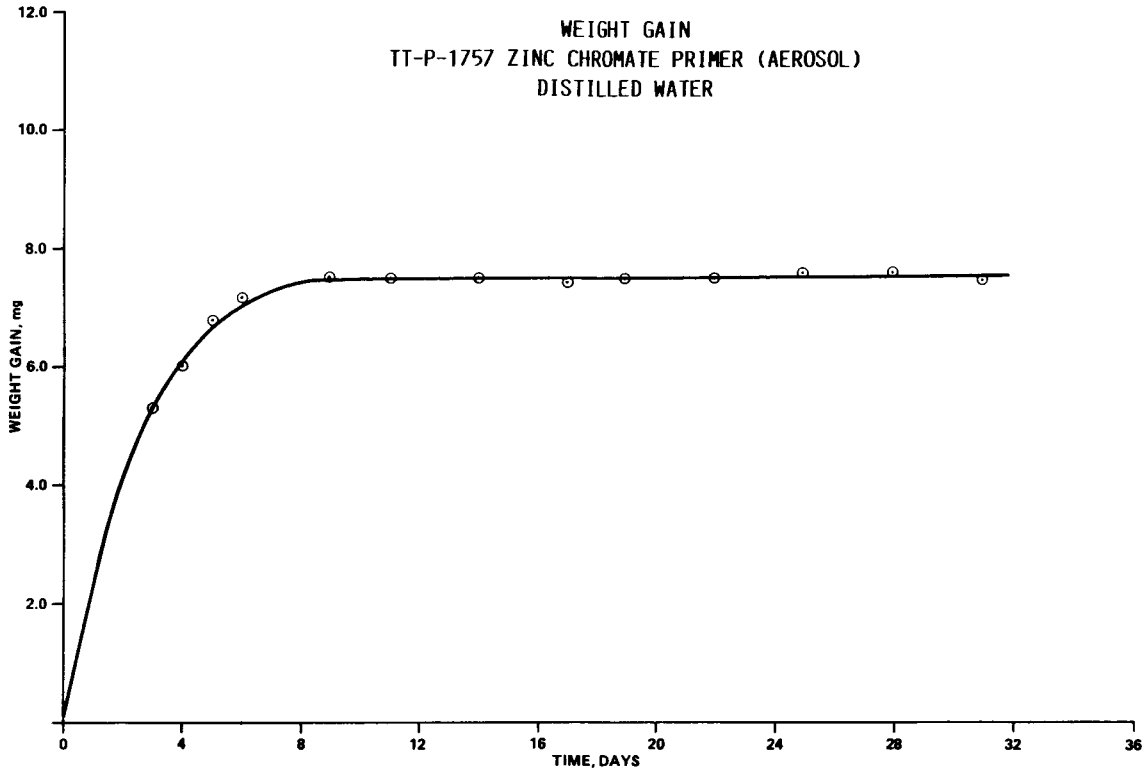

Figure 13. Weight gain-time curve for TT-P-1757 aerosol primer immersed in distilled water.

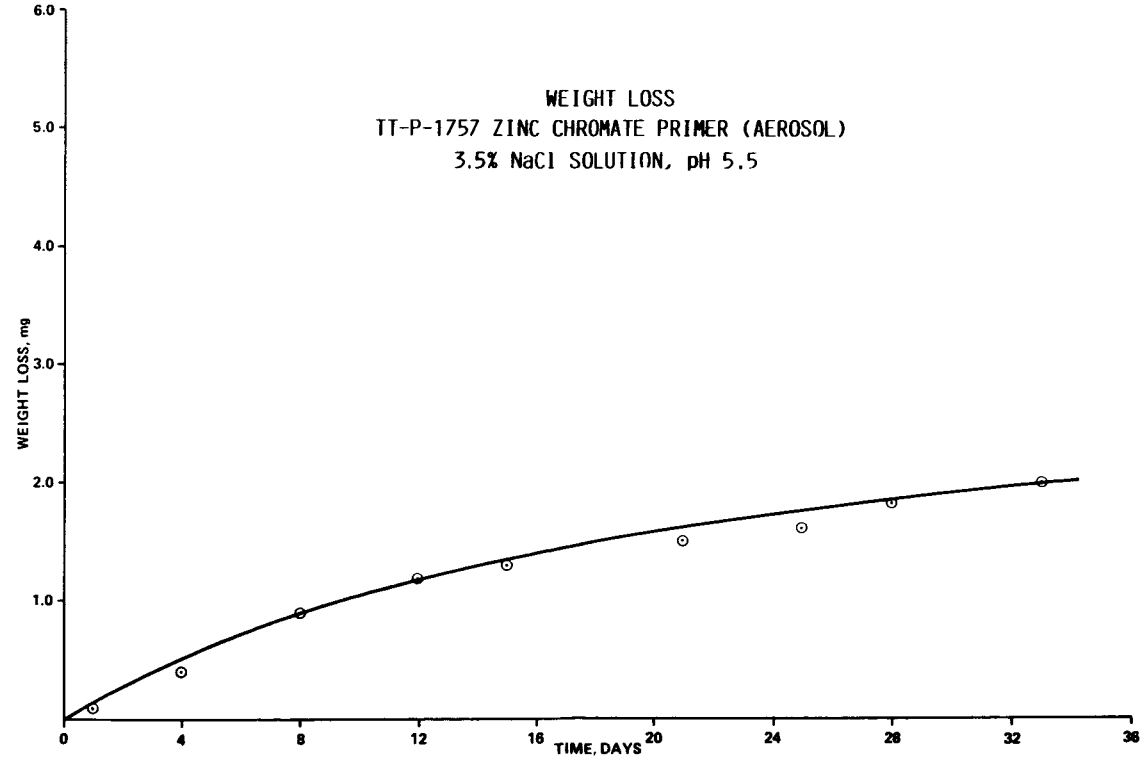

Figure 14. Weight loss-time curve for the TT-P-1757 aerosol primer immersed in 3.5 percent NaCl solution at pH 5.5.

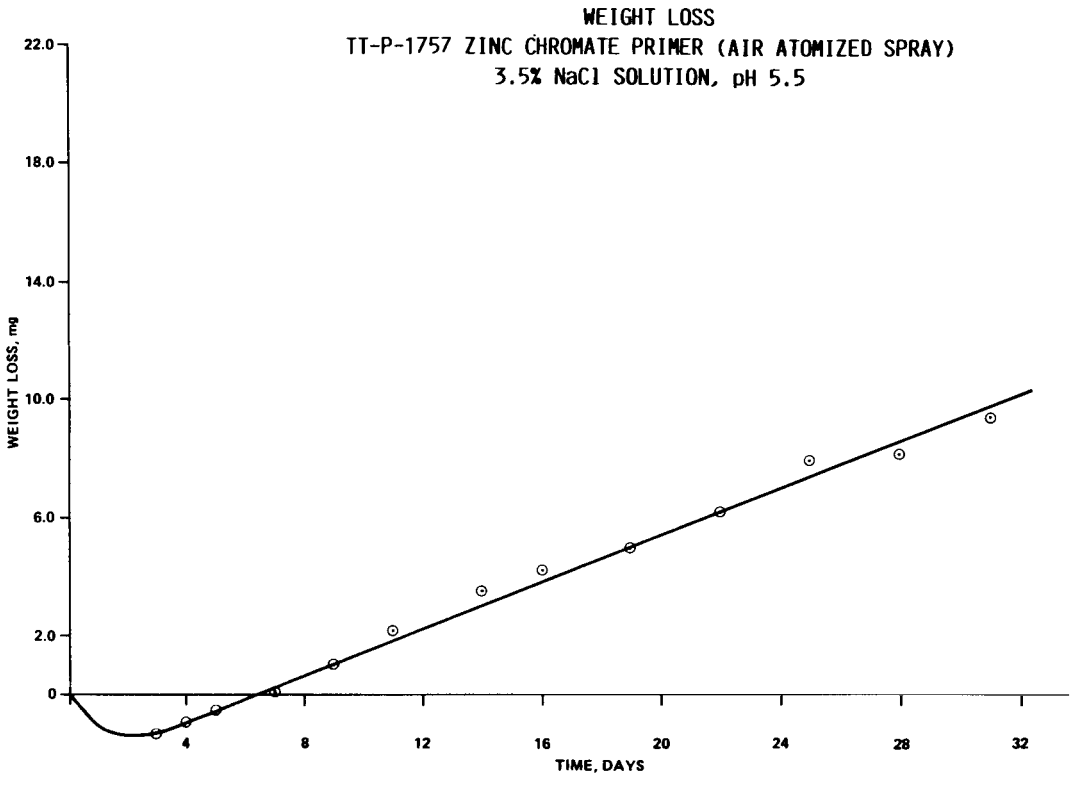

Figure 15. Weight loss-time curve for the TT-P-1757 air atomized primer immersed in 3.5 percent NaCl solution at pH 5.5.

Correlation of Experimental Corrosion Rate-Time Curves with the Corrosion Mechanism for Aluminum

A thorough study of the mechanism of inhibitive chromate primers, as well as the mechanism of aluminum corrosion has been made by Boies and McDonald [8]. The mechanism of corrosion inhibition by zinc chromate involves polarization of cathodic sites by precipitation of a complex material, such as chromic chromate or zinc tetroxychromate to prevent hydrogen evolution, preventing the spread of corrosion and allowing natural processes to heal the anodic site.

For the corrosion of aluminum, the painted aluminum may be considered as a voltaic cell, with the aluminum metal as the anode, separated from the paint film, which acts as the cathode compartment, by an inner layer of amorphous Al_2O_3 and an outer layer of crystalline hydrated oxide, probably $Al_2O_3.3H_2O$ at room temperature. The outer bulk layer is porous and does not afford protection, while the layer of amorphous aluminum oxide is the limiting factor in the corrosion process. Electrons pass across this barrier layer fairly readily, but the diffusion of aluminum ions across this layer is slow and, according to the previous investigators, growth of the barrier layer stops at a thickness depending on the driving force or cell potential, E_{cell}. The anodic reaction is:

(1) $Al = Al^{+3} + 3e$ $\qquad E° = 1.66$ V

for which:

$$E = E^\circ - \frac{0.0592}{3} \log [Al^{+3}]$$

Two cathodic reactions are possible:

(2) $2H_2O+O_2+4e = 4OH^-$ $\qquad E^\circ = 0.401$ V

for which:

$$E = E^\circ = 0.0592 \log[OH^-] + \frac{0.0592}{4} \log [O_2]$$

The second possible reaction is:

(3) $2H_2O+2e = 2OH^-+H_2$ $\qquad E^\circ = 0.828$ V

for which:

$$E = E^\circ - 0.0592 \log [OH^-]$$

The overall reaction involving reaction (2) is:

(4) $4Al+3O_2+6H_2O=4Al(OH)_3$ $\qquad E^\circ_{cell} = 2.06$ V

For reaction (3) the overall reaction is:

(5) $2Al+6H_2O = 6Al(OH)_3+3H_2$ $\qquad E^\circ_{cell} = 0.832$ V

From reactions (4) and (5) it is clear that reaction (4) will occur most readily, with both water and oxygen being required for the reaction to take place, while only water is required for reaction (5), the hydrogen evolution reaction. The initial reaction, therefore, proceeds according to equation (4), slowed by the presence of inhibitor. The concentration of hydroxyl ions is probably fairly constant, since the aluminum ions react with hydroxyl ions to form insoluble $Al(OH)_3$ initially, with the hydroxyl ion concentration being limited according to the solubility product for $Al(OH)_3$. The rate is most likely limited by the diffusion of oxygen to the cathodic sites. As long as oxygen is available, reaction (4) proceeds normally, while the thickness of the barrier layer remains constant, unless disturbed by other

factors, such as dissolution of the film at low or high pH (Al_2O_3 is soluble in either acids or alkalis). The amorphous aluminum oxide slowly hydrates to form the porous, crystalline bulk layer, while more aluminum ions diffuse out to maintain the thickness of the barrier layer. According to the proposed mechanism, the thickness of the barrier layer depends on the driving force, or E_{cell}, of the film formation. The overall rate of reaction (4) is no doubt governed by the rate of decrease in both oxygen concentration and the rate of thinning of the barrier layer, due either to dissolution by the electrolyte solution or to a decrease in the cell voltage. The oxygen concentration is probably depleted faster than the thickness of the barrier layer, so that reaction (4) is slowed more by the lack of oxygen than it is increased by a decrease in thickness of the barrier layer. This is consistent with the corrosion rate-time curves obtained in the present study, where a small decrease in the corrosion rate occurred during the first few days. As the oxygen concentration becomes smaller, E_{cell} for reaction (4) is decreased, and reaches a point where reaction (5) becomes the dominating reaction. Evidence that the rapid hydrogen evolution reaction occurs was given by the presence of blisters under the paint films for samples used in this work. The amorphous layer also is thinner at this point, so that diffusion of aluminum ions through the barrier layer is more rapid. The corrosion rate therefore increases rapidly. When reaction (5) is dominant, the thickness of the barrier layer is thus reduced, and could result in catastrophic failure under the paint film. However, the experimental results show that a maximum corrosion rate is reached, after which the corrosion rate slows. This suggests that thinning of the amorphous layer by dissolution of amorphous aluminum oxide may be of comparable importance to the driving force of the chemical reaction. This is consistent with the fact that aluminum corrodes more rapidly in solutions of low and high pH. Also, the solubility of aluminum oxide is enhanced by high ionic strength solutions, consistent with the fact that corrosion is more rapid in solutions with high chloride content, such as the 3.5 percent NaCl solution employed in this work. The thickness of the amorphous layer is clearly increased during the rapid hydrogen evolution reaction, so that the corrosion rate again slows due to the slowed diffusion of ions across the amorphous layer. The corrosion rate can reach a point where oxygen diffusion is again significant and the corrosion process can again proceed by reaction (5). Although polarization resistance measurements were, in most cases, difficult to make toward the end of the 30 day test period, indications were that the corrosion rates were again increasing. Variation of the corrosion rate with time under the paint film, therefore, may be cyclic in nature, with the initial processes being repeated frequently. Evidence for a second peak appeared for the DeSoto 515-346 primer shown in Figure 8, where the first peak appeared at a fairly early time (11 days). The concentration of inhibitor is gradually depleted due to leaching by the electrolyte solution, and, as with the aluminum oxide, solubility is increased in solutions with high ionic strength. The amplitudes and frequencies of the corrosion rate cycles, therefore, might increase with time, giving rise to higher overall corrosion rates, unless the corrosion rates are limited by other factors.

Primers of Special Interest to the Space Shuttle Transportation System

The normalized resistance-time for corrosion rate-time curves for the External Tank primer currently in use are shown in Figure 8. The resistance-time curves for thicknesses of 15.2 μm and 35.6 μm both show rather sharp drops, indicating that water is taken up rather rapidly in both cases. The water uptake is similar, in general, to that for the TT-P-1757 aerosol primer. The corrosion rate-time curve for the 15.2 μm thickness shows a maximum at 11 days, with evidence for a second maximum at 25 days. The appearance of the first maximum, which probably marks the onset of the hydrogen evolution reaction and the beginning of general destruction of the protective properties of the paint, occurs at an earlier time than that in any of the other primers investigated (14 to 16 days). A possible explanation may be that this primer is less permeable to oxygen than the other primers. For the 35.6-μm thickness, the corrosion rate was not measurable until day 11, with the mean corrosion rate for days 11 to 28 being only 0.0015±0.0005 mpy, while that for the 15.2-μm thickness was 0.017±0.0025 mpy for days 3 to 27. Evidence for a small peak occurred at day 21 for the 35.6-μm thickness.

The normalized resistance-time and corrosion rate-time curves for the primer previously used for the External Tank (DeSoto 513-007) are shown in Figure 9. Although the resistance remains high throughout the 30 day period, the initial drop is probably significant, since sufficient water was taken up to permit measurement of the corrosion rate. The mean corrosion rate for days 2 to 16 was 0.0277± 0.0080, quite a bit higher than that for the new primer (0.017±0.0025). Also, the thickness of this coat (17.8 μm) is greater than that for the new primer to which it is compared (15.2 μm). The peak maximum, marking the onset of the hydrogen evolution reaction, occurs at day 14.

The electrical resistance-time and corrosion rate-time curves for Bostik 463-6-3 epoxy calcium chromate primer, the primer presently used for the Solid Rocket Boosters, are shown in Figure 10. The normalized resistance does not begin to drop appreciably until day 15, after which it drops rather rapidly to a low value. This indicates that the paint film is relatively impermeable to water. The corrosion rate did not become measurable until day 18, after which it remained at a relatively low value, with evidence for a small peak occurring at about day 24. The mean corrosion rate for days 18 to 32 was 0.0012± 0.0002 mpy. This primer appears extremely good from the standpoint of corrosion protection, although nothing can be said, from these measurements, about adhesive properties or ability to withstand cryogenic or elevated temperatures.

CONCLUSIONS

Electrical resistance-time measurements provide valuable information concerning the porosity of paint films, but also depend a great deal on their thickness. For comparative purposes, paint films of approximately the same thickness should be used. Corrosion rate-time curves for painted metals give a great deal of insight into the corrosion mechanism. Corrosion rates for 2219-T87 aluminum, coated with various inhibitive primers, had values generally less than 0.2 mpy. This is to be compared with the corrosion rate for the bare metal in the same solution (3.5 percent NaCl at pH 5.5), for which the corrosion rate is approximately 16 mpy. The corrosion rate-time curves at pH 5.5 are generally characterized by a peak, which occurred usually at around 14 to 16 days. The incidence of the first peak is attributed, according to the proposed mechanism, to the beginning of the hydrogen evolution reaction and the beginning of general destruction or deterioration of the protective properties of the paint coating. It is proposed from these studies that the variation of the corrosion rate with time may be cyclic in nature, and in one instance there is evidence that a second peak occurs. However, the nature of the corrosion rate-time curves may be different at higher pH values. Aluminum is amphoteric in nature, and the corrosion rate for bare aluminum is high at very low and very high pH values, exhibiting a minimum at about pH 8.0 (approximately the pH of seawater). Studies at higher pH may provide more insight into the overall corrosion mechanism and may help to definitely establish whether dissolution of the amorphous Al_2O_3 layer by the surrounding medium or the driving force of the corrosion reaction is the more important factor in the corrosion process.

It was found in these studies that the value of the polarization resistance (R_p) depends very much on the thickness of the paint film. In every instance where more than one thickness was used, values of R_p were higher for the thicker paint films. This result is in contradiction with that for a previous study [4], where the values of R_p were said to be independent of the thickness. This difference might be caused by the fact that R_p was determined in the previous study from the slope of the voltage-current curve polarized over a wide range (±100 mV from the rest potential) and not by taking the derivative as indicated in equation (2).

Computer calculation of the appropriate parameters, using programs such as PϕLCURR, is essential for accurate determination of the corrosion rate-time curves. As described previously, the R_p values display no significant deviations from their mean values over rather broad time spans, so that the values of the corrosion rates depend greatly on the shapes of the curves obtained in the polarization resistance scans. Therefore, the Tafel slopes, as obtained in the least squares fit of the experimental data, play an important role in determining the corrosion rates. Also, it is essential that the observed data be corrected for the ohmic drop due to the high resistances of the paint films. This was carried out in the present study.

In contrast to the study of painted steel by Wornwell and Brasher [2], the variation of corrosion potentials with time for painted aluminum generally showed no significant variations from their mean values with time. Only in one instance (DeSoto 511-300 Epoxy Molybdate), where a very thick primer coating was employed (53.3 μm), did the corrosion potential-time curve show a significant drop (-230 mV to -800 mV at 26 days). This implies that the measurement of corrosion potentials might be useful in cases where the corrosion potential of the painted aluminum is significantly different from that of the bare metal, as for thick primer coats or for primer-topcoat combinations.

Future work will include the study of corrosion rates at higher pH values for at least one primer. Also, the effect of exposure to cryogenic and elevated temperatures, both before and after water uptake by the paint film, will be investigated. In addition, AC impedence techniques, from which values of R_p, R_Ω and capacitance may be obtained, might be useful for studying very thick paint coats, such as primer-topcoat combinations where traditional DC methods might fail. Actual corrosion rates cannot be obtained using this technique, but the corrosion rate is inversely proportional to R_p. This method makes use of only very small signals which do not disturb the electrode properties to be measured.

REFERENCES

1. Wolstenholme, J.: Electrochemical Methods of Assessing the Corrosion of Painted Metals – A Review. Corrosion Science, Vol. 13, 1973, p. 521.

2. Wormwell, F. and Brasher, D. M.: J. Iron Steel Inst., Vol. 162, 1949, p. 129.

3. Yakubovitch, S. V., Nitsberg, L. V. and Karyakina, M. I.: Proc. 6th Int. Conf. Electrodepos., 1964, p. 321.

4. Bureau, M.: Corros. Trait Prot. Finish, Vol. 16, 1968, p. 235.

5. Rozenfel'd, I. L., Oshe, E. L., and Akimov, A. G.: Korroziya Metallov i Splavov, N. L. L. translation, Metallurgizdat, Moscow, 1965, p. 302.

6. Mansfeld, F.: The Effect of Uncompensated IR-Drop on Polarization Resistance Measurements. Corrosion, Vol. 32, 1976, p. 143.

7. Gerchakov, S. M., Udey, L. R., and Mansfeld, F.: An Improved Method for Analysis of Polarization Resistance Data. Corrosion, Vol. 37, 1981, p. 696.

8. Boies, D. B. and McDonald, W. P.: Mechanism of Inhibitive Chromate Primers, Report. No. IITRI-U6047-8. IIT Research Institute, Technology Center, Chicago, Illinois 60616, 1968.

1. REPORT NO.	2. GOVERNMENT ACCESSION NO.	3. RECIPIENT'S CATALOG NO.
NASA TP-2459		

4. TITLE AND SUBTITLE	5. REPORT DATE
An Electrochemical Study of the Corrosion Behavior of Primer Coated 2219-T87 Aluminum	April 1985
	6. PERFORMING ORGANIZATION CODE
7. AUTHOR(S)	8. PERFORMING ORGANIZATION REPORT #
Merlin D. Danford and Ralph H. Higgins	
9. PERFORMING ORGANIZATION NAME AND ADDRESS	10. WORK UNIT NO.
George C. Marshall Space Flight Center Marshall Space Flight Center, Alabama 35812	M-483
	11. CONTRACT OR GRANT NO.
	13. TYPE OF REPORT & PERIOD COVERED
12. SPONSORING AGENCY NAME AND ADDRESS	Technical Paper
National Aeronautics and Space Administration Washington, D.C. 20546	14. SPONSORING AGENCY CODE

15. SUPPLEMENTARY NOTES

Prepared by Materials and Processes Laboratory, Science and Engineering Directorate

16. ABSTRACT

The corrosion behavior for 2219-T87 aluminum coated with various primers, including those used for the External Tank and Solid Rocket Boosters of the Space Shuttle Transportation System, has been investigated using electrochemical techniques. Corrosion potential-time, polarization resistance-time, electrical resistance-time, and corrosion rate-time measurements were all investigated. It was found that electrical resistance-time and corrosion rate-time measurement were most useful for studying the corrosion behavior of painted aluminum. Electrical resistance-time determinations give useful information concerning the porosity of paint films, while corrosion rate-time curves give important information concerning overall corrosion rates and corrosion mechanisms. In general, the corrosion rate-time curves all exhibited at least one peak during the 30 day test period, which was attributed, according to the proposed mechanisms, to the onset of the hydrogen evolution reaction and the beginning of destruction of the protective properties of the paint film.

17. KEY WORDS	18. DISTRIBUTION STATEMENT
Electrochemical Methods Primer-Coated Aluminum Corrosion Mechanisms Primer Evaluation	Unclassified - Unlimited Subject Category 26

19. SECURITY CLASSIF. (of this report)	20. SECURITY CLASSIF. (of this page)	21. NO. OF PAGES	22. PRICE
Unclassified	Unclassified	26	A03

For sale by National Technical Information Service, Springfield, Virginia 22161

NASA-Langley, 1985